

Antenna with a Reactive Impedance Substrate for Mine Rescue Applications

Martin Roestorff¹, Johann W. Odendaal¹, Johan Joubert¹

¹ Centre for Electromagnetism, University of Pretoria, Pretoria 0002, South Africa; Corresponding author: wimpie@up.ac.za

ABSTRACT—Two electrically small, RIS backed, antennas are presented that can be used by rescue workers to locate miners in emergency situations in underground mines. One antenna was designed for optimum impedance bandwidth and the other for compact size, with at least 5% impedance bandwidth. At 433 MHz both antennas have maximum gain values above 5 dBi, and both antennas radiate on average at least 10 dB more power in the front hemisphere than in the rear hemisphere, to reduce interaction with the wearer and aid in locating the missing miners. The first antenna, a planar monopole antenna with RIS backplane had a -10 dB reflection coefficient bandwidth of 25.1 %, and a form factor of $0.4 \lambda_0$ by $0.4 \lambda_0$ by $0.069 \lambda_0$. The second antenna, a loaded planar monopole antenna with RIS backplane had a -10 dB reflection coefficient bandwidth of 5.3 %, and a form factor of $0.346 \lambda_0$ by $0.346 \lambda_0$ by $0.107 \lambda_0$. Measured and simulated results for the two antennas are presented.

Keywords: Reactive impedance surfaces, wearable antennas, compact antennas.

1. INTRODUCTION

RFID systems operating in the 433 MHz band are commonly used in underground mines to keep track of personnel, equipment and supplies. Miners typically carry passive or low-powered RFID systems on their person that communicates with tracking systems in the mine. These tracking systems let the user know how many miners are underground, where they have been working, and where they are currently located. In an emergency where miners get trapped or lost underground, these tracking systems help by giving rescuers the last known location of the miners. Once the search has commenced, the rescuers can employ a system that actively communicate with the RFID systems on the lost or trapped miners, thereby allowing the rescuer to ascertain where the miners are relative to their own position. A possible solution would include a directional antenna that can be worn by the rescuer while they are looking for the trapped miners [1].

Antenna miniaturization has allowed for the realization of antennas small enough to be considered wearable at increasingly lower frequencies, the possible applications for body area networks (BAN's) have increased. BAN's, which can allow for wireless communication between different subsystems located on a single human, as well as allowing wireless intrapersonal links between a BAN and remote systems, can now be implemented over an ever-increasing range of frequencies [2, 3]. This has led to the development of more and more antennas that can be used whilst being worn by a human. It has however been shown that human loading, due to the proximity between an antenna worn by a human and the human in question, can have an adverse effect on antenna performance [4, 5].

The antenna in [3] managed to solve the human loading issues in the 2.4 GHz medical band. This antenna made use of an Artificial Magnetic Conductor (AMC), which has been known to enable

antenna miniaturization as well as bandwidth improvements [6, 7]. A reactive impedance surface (RIS) was used in [8] to decrease the size, and increase the bandwidth, of a patch antenna in the frequency range of 420 MHz to 450 MHz. This antenna was designed to have a directional radiation pattern, and to be insensitive to platform effects when mounted on a vehicle. The RIS was designed on a low loss ceramic with a dielectric constant of 10.2. This antenna had high manufacturing costs due to the use of expensive materials, and made use of a complex RIS design.

This paper investigates the use of a RIS to improve the wear ability of an antenna designed to operate at 433 MHz. A possible application for the antenna designs presented in this study is direction finding in underground mines. The antenna can be worn by a rescue worker searching for a trapped miner by looking for the miner's RFID tag. The proposed antennas use only widely available, low cost materials with basic designs to achieve the same quality of results that has previously been achieved using highly specialized materials and complex designs.

2. ANTENNA GEOMETRY AND DESIGN

The square patch RIS presented in [7] was used as a starting point in the design of the RIS for this study. The unit cell in Fig. 1 was simulated with CST Microwave Studio [9] as part of an infinitely periodic structure and equations were derived for the design parameters indicated in Fig. 1 to allow the RIS to be easily scalable in center frequency and dielectric constant of the material.

The design equations are:

$$L = \lambda/4 \quad (1)$$

$$g = \lambda/11 \quad (2)$$

$$h = \lambda/6 \quad (3)$$

$$d = \lambda_0/50 \quad (4)$$

where λ_0 is the wavelength in free space, λ is the wavelength in the dielectric medium, L is the length of the sides of a square patch, g is the distance between patches, h is the height of the unit cell, and d is

the distance between the unit cell and the reference plane. These equations were used to design a unit cell that has a 0° phase reflection at 433 MHz, shown in Fig. 2, using an FR-4 model with a dielectric constant of 4.6 and a loss tangent of 0.02. A two by two square patch RIS was used as a reflector for the planar monopole antenna, with the goal of radiating most of the antenna's power away from the wearer. The RIS of the final design was 38.4 mm thick.

A planar monopole antenna was designed with a -10 dB reflection coefficient bandwidth of 9.2 %, and an omnidirectional radiation pattern. Two different integrated antennas were developed: the first, a standard planar monopole antenna, was designed for optimal VSWR bandwidth performance, and the second antenna, a loaded planar monopole antenna, was designed to be as compact as possible. The standard planar monopole antenna was designed to have a reflection coefficient smaller than -10 dB, and a maximum gain of more than 5 dBi, over as wide a frequency band as possible. The loaded planar monopole antenna was designed to be as compact as possible whilst retaining practical performance, i.e. a -10 dB reflection coefficient bandwidth of at least 5 %, and a maximum gain value of at least 5 dBi at 433 MHz.

The design parameters for the standard planar monopole antenna are shown in Fig. 3 and listed in Table I. The total length and width of the standard planar monopole antenna is 277.29 mm, ($0.4 \lambda_0$), and the total height of the integrated antenna is 48 mm, ($0.069 \lambda_0$). Optimizing the width of the monopole (loaded monopole) to further minimize the size of the antenna, resulted in a total length and width of 239.39 mm ($0.346 \lambda_0$). The total height of the loaded planar monopole antenna was slightly larger than that of the standard planar monopole antenna, although at 74 mm ($0.107 \lambda_0$) it is still compact. Fig. 4 shows the design and indicates the design parameters of the loaded planar monopole antenna, and Table II lists the values of the final loaded planar monopole antenna. Changes in impedance characteristics, due to design parameter modifications in both the standard planar monopole and loaded planar monopole antennas, are compensated for by modifying the impedance characteristics of the RIS slot.

3. EXPERIMENTAL VALIDATION

The antenna prototypes were manufactured and the measured results were compared with the results obtained in simulation. Fig. 5 (a) shows a picture of the standard planar monopole antenna and the measured reflection coefficients for the standard planar monopole antenna are compared with the simulated results in Fig. 5 (b). The -10 dB reflection coefficient bandwidth for the standard planar monopole antenna was measured at 25.1 %. A slight shift in frequency can be observed between the simulated and measured reflection coefficients. Fig. 6 compares the measured and simulated principle plane radiation patterns of the standard planar monopole antenna. The vast majority of power is radiated forward, and the standard planar monopole antenna provides good cross polarization performance. Fig. 7 shows that the boresight gain of the standard planar monopole antenna is consistently higher than 5 dBi. The front to back power ratio was calculated from the radiation patterns as the ratio between the average power radiated towards the front hemisphere, relative to the average power radiated towards the rear hemisphere. The front to back power ratio is approximately 10 dB at 433 MHz.

The effects of human loading on antenna performance were investigated through simulation, based on the model in [3]. The model for human tissue was simulated with the properties listed in Table III, and the configuration shown in Fig. 8. Simulations were performed with a distance of 0.1 mm, 20 mm and 40 mm between the antenna and the human tissue. The width and length of the human tissue model was kept at double the width and length of the antenna. The effects of human loading on the boresight gain of the standard planar monopole antenna and reflection coefficient is shown in Fig 9. The simulated results show that both the 5 dBi gain bandwidth and the -10 dB impedance bandwidth decreased slightly, and that the 5 dBi gain bandwidth shifted to a slightly higher frequency range.

The loaded planar monopole antenna is shown in the anechoic chamber in Fig 10 (a) and achieved a -10 dB reflection coefficient bandwidth of 5.28 %, Fig. 10 (b). Fig. 11 shows the agreement between the simulated and measured radiation patterns for the loaded planar monopole antenna. The measured boresight gain at 433 MHz is higher than 5 dBi, and the front to back power ratio is again higher than 10 dB, as shown in Fig. 12. The effects of human loading on the boresight gain of the loaded planar

monopole antenna and reflection coefficient is shown in Fig 13. The 5 dBi gain bandwidth decreased slightly at the lower frequencies. The reflection coefficient bandwidth decreased approximately 5 MHz for 20 mm separations between the antenna and tissue, and increased approximately 5 MHz for a 0.1 mm separation, relative to no loading. At 40 mm separation, the reflection coefficient bandwidth is approximately the same as with no loading.

4. CONCLUSION

Two antennas were designed, simulated and manufactured as wearable antennas for rescuers to locate lost or trapped miners in underground mines. The first of the two antennas, the standard planar monopole antenna with RIS reflector, was designed for optimal impedance bandwidth performance. At 433 MHz it radiated on average 10 dB more power towards the front hemisphere than the rear hemisphere, and it had a boresight gain higher than 5 dBi at the center frequency. The antenna has a -10 dB reflection coefficient bandwidth of 25.1% and a form factor of $0.4 \lambda_0$ by $0.4 \lambda_0$ by $0.069 \lambda_0$.

The second antenna, a loaded planar monopole antenna, was designed as compact as possible: $0.346 \lambda_0$ by $0.346 \lambda_0$ by $0.107 \lambda_0$, with a -10 dB reflection coefficient bandwidth of 5.28 % and a front to back power ratio of 10 dB. The high front to back power ratio for both antennas make them suitable as wearable antenna for mine rescue applications.

ACKNOWLEDGMENT

The authors are grateful for the assistance provided by B. Jacobs from SAAB, South Africa and L. Lindeboom from Gerotek with the radiation pattern measurements. This work is based on the research supported by the National Research Foundation (NRF) of South Africa (Grand Number 114941).

REFERENCES

1. A. S. Bhat, B. Raghavendra and G. N. Kumar, "Enhanced Passive RFID Based Disaster Management for Coal Miners," *International Journal of Future Computer and Communication*, vol. 2, no. 5, pp. 476-480, 2013.
2. I. M. S. ul Huque, K. S. Munasinghe, M. Abolhasan and A. Jamalipour, "SEA-BAN: Semi-autonomous adaptive routing in wireless body area networks," in *2013 7th International Conference on Signal Processing and Communication Systems (ICSPCS)*, Carrara, VIC, 2013.
3. Z. H. Jiang, D. E. Brocker, P. E. Sieber and D. H. Werner, "A Compact, Low-Profile Metasurface-Enabled Antenna for Wearable Medical Body-Area Network Devices," *IEEE Antennas and Propagation*, vol. 62, no. 8, pp. 4021-4030, August 2014.
4. A. Michalopoulou, A. Alexandridis, T. Zervos and F. Lazarakis, "A wearable multiband monopole antenna for digital television and wireless communications," in *2014 8th European Conference on Antennas and Propagation (EuCAP)*, The Hague, Netherlands, 2014.
5. M. Paulides, J. Bakker, N. Chavannes and G. van Rhooen, "A Patch Antenna Design for Application in a Phased-Array Head and Neck Hyperthermia Applicator," *IEEE Transactions on Biomedical Engineering*, vol. 54, no. 11, pp. 2057 - 2063, November 2007.
6. J. Joubert, J. Vardaxoglou, W. Whittow and J. Odendaal, "CPW-Fed Cavity-Backed Slot Radiator Loaded With an AMC Reflector," *IEEE Transactions on Antennas and Propagation*, vol. 60, no. 2, pp. 735-742, February 2012.
7. H. Mosallaei and K. Sarabandi, "Antenna Miniaturization and Bandwidth Enhancement Using a Reactive Impedance Substrate," *IEEE Transactions on Antennas and Propagation*, vol. 52, no. 9, pp. 2403-2414, 2004.
8. K. Sarabandi, A. M. Buerkle and H. Mosallaei, "Compact Wideband UHF Patch Antenna on a Reactive Impedance Substrate," *IEEE Antennas and Wireless Propagation Letters*, vol. 5, no. 1, pp. 503-506, 2006.
9. CST STUDIO SUITE® 2016, CST AG, Germany, www.cst.com.

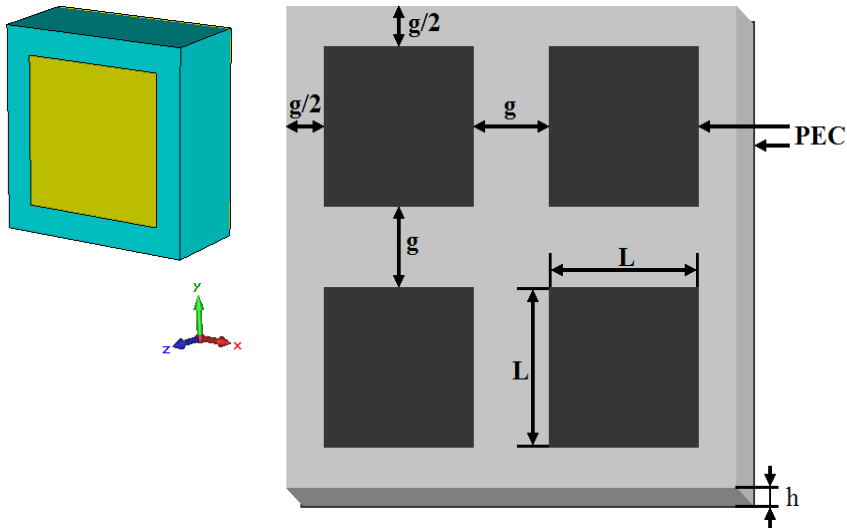


Fig. 1. Square patch RIS and unit cell.

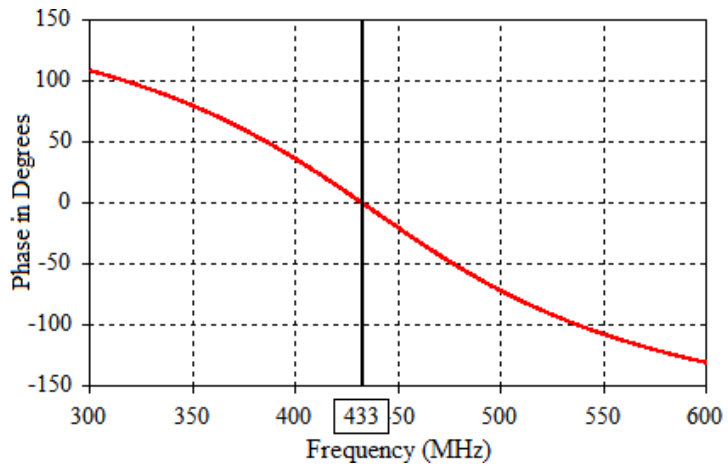


Fig. 2. Square patch RIS unit cell reflection coefficient phase.

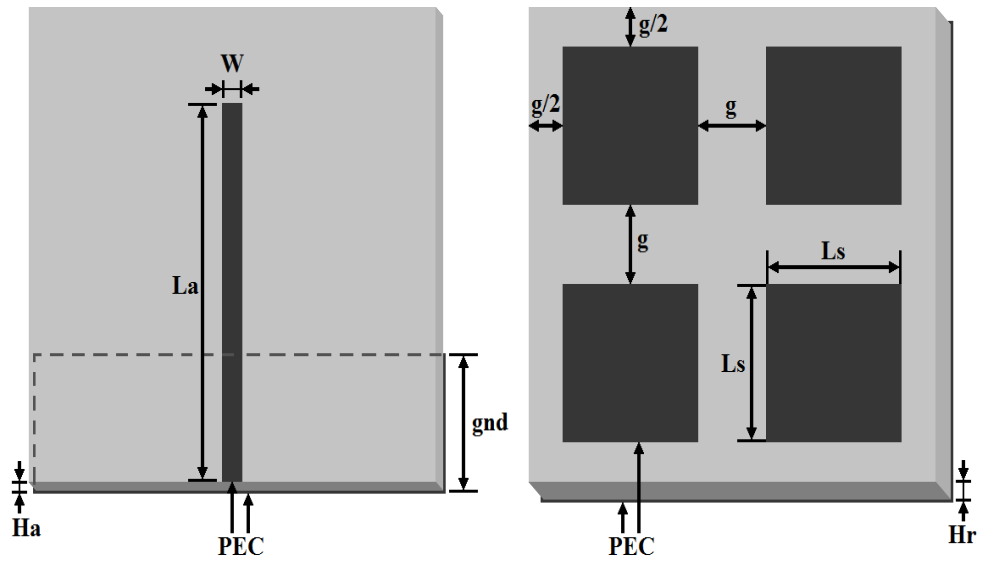


Fig. 3. Standard planar monopole antenna design parameters.

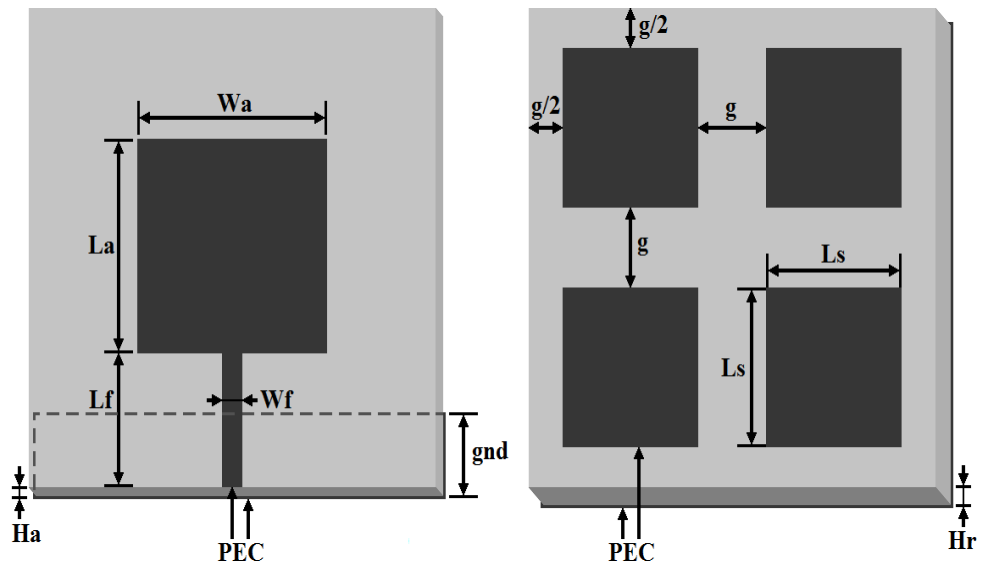


Fig. 4. Loaded planar monopole antenna design parameters.

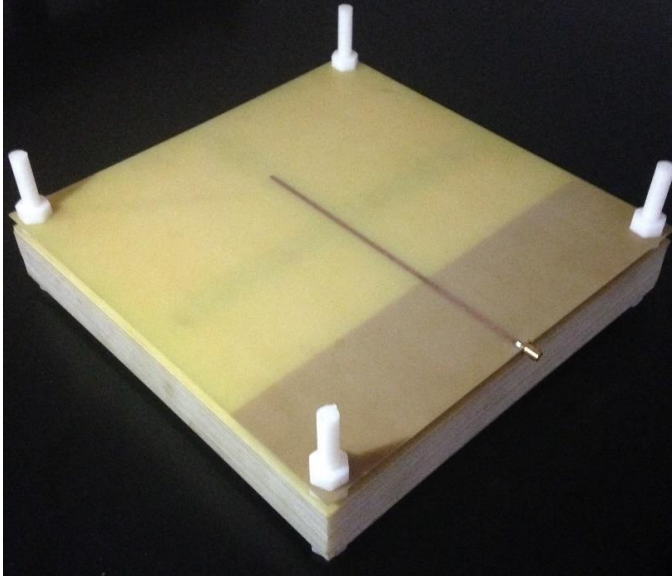


Fig. 5. (a) A picture of the standard planar monopole antenna.

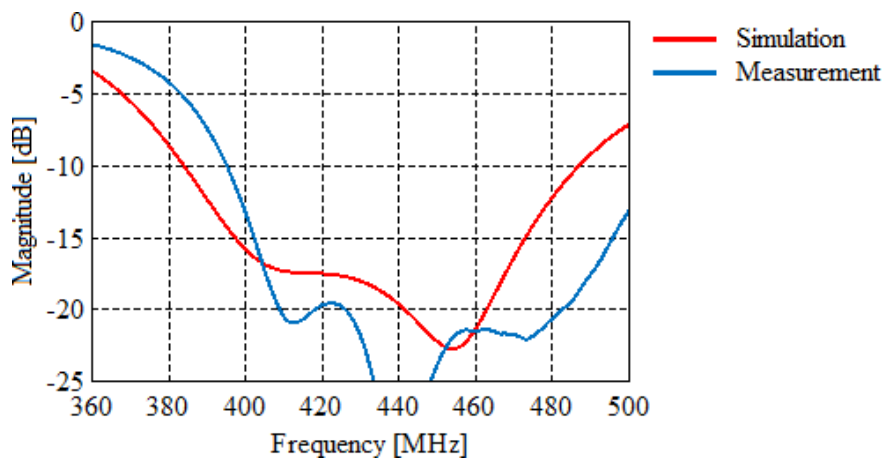


Fig. 5. (b) A comparison between the measured and simulated reflection coefficients for the standard planar monopole antenna.

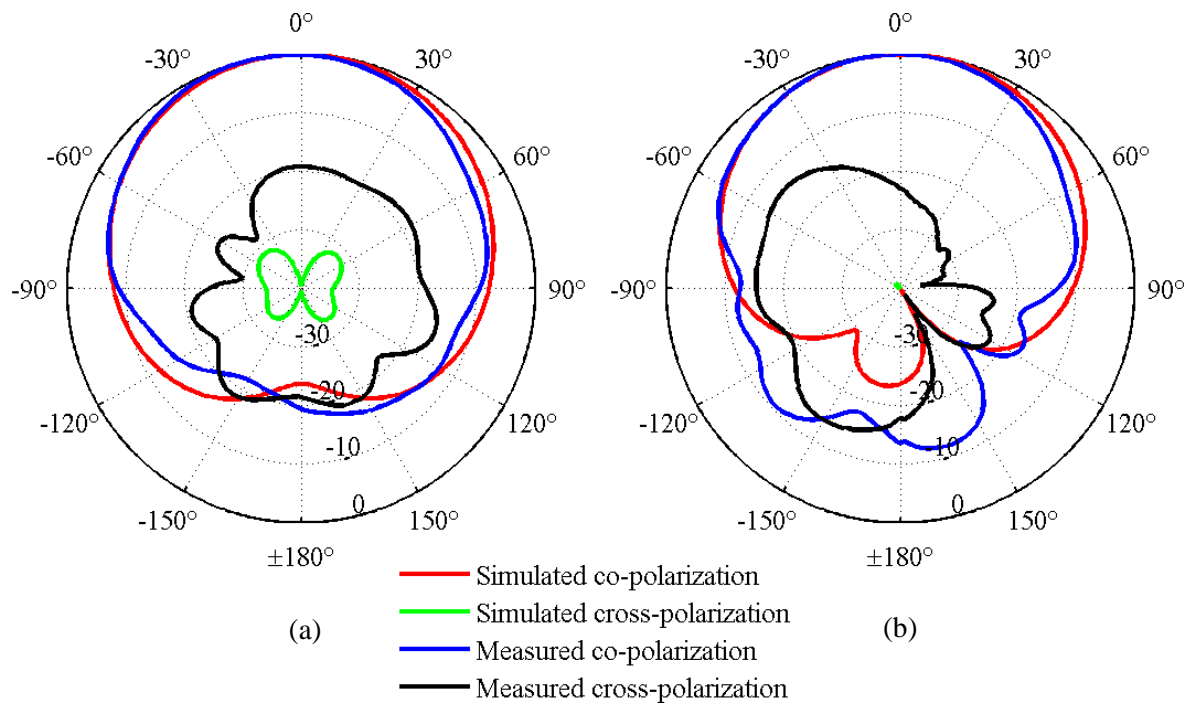
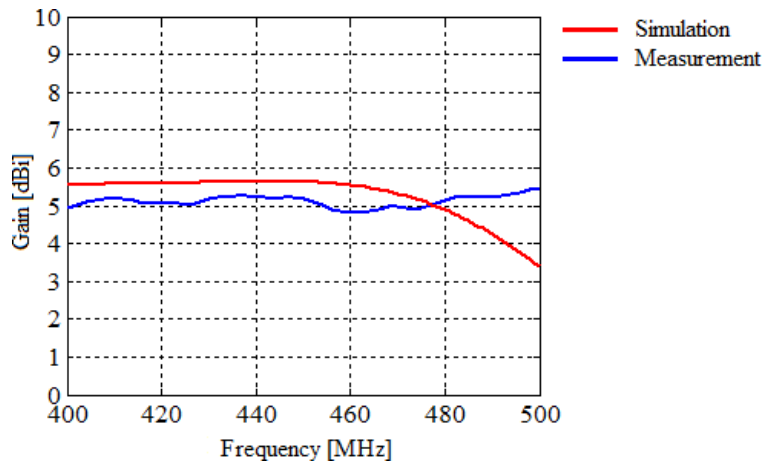
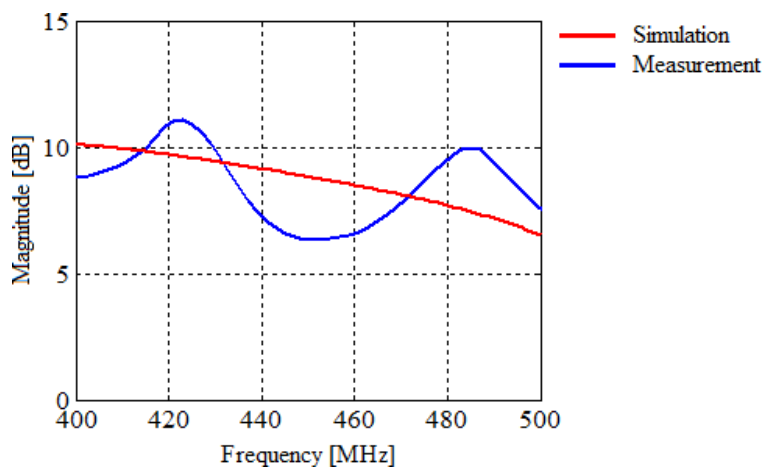


Fig. 6. Measured and simulated normalized radiation patterns for the standard planar monopole antenna, (a) H-plane and, (b) E-plane radiation patterns.



(a)



(b)

Fig. 7 (a). Measured and simulated boresight gain and (b) front to back power ratio for the standard planar monopole antenna. The front to back power ratio is calculated as the ratio between the average power radiated towards the front hemisphere, relative to the average power radiated towards the rear hemisphere.

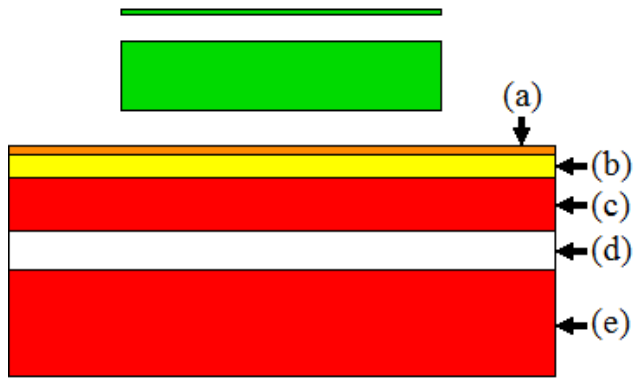
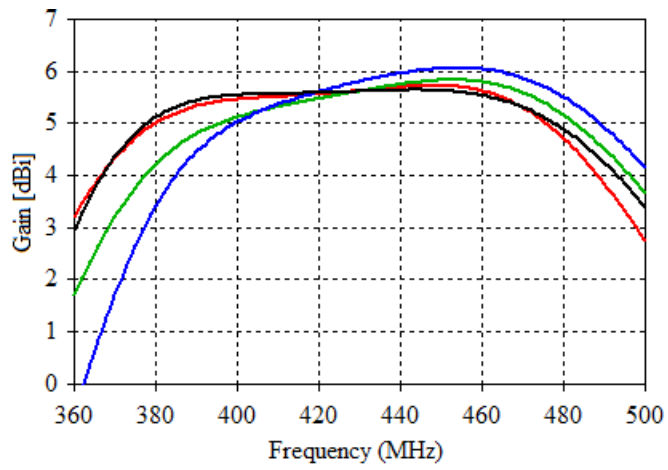
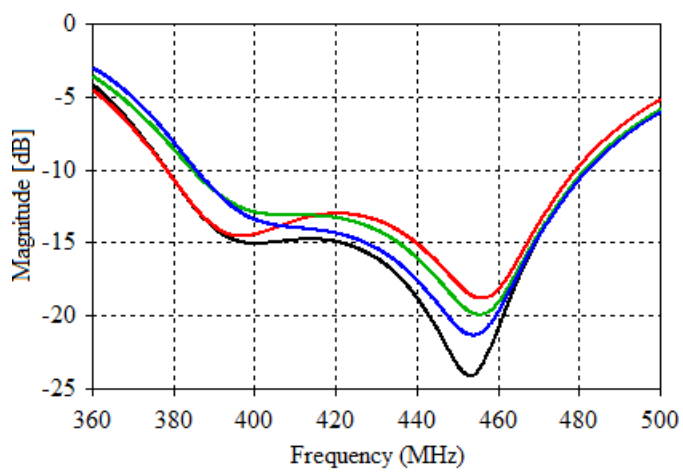


Fig. 8. Human loading simulation model, based on the model from [3]. The antenna is at the top and the simulated human is at the bottom. The width and length of the human tissue model was kept at double that of the antenna. (a) Skin. (b) Fat. (c) Muscle layer 1. (d) Bone. (e) Muscle layer 2.



(a)



(b)

- human distance = 0.1 mm
- human distance = 20.0 mm
- human distance = 40.0 mm
- no human tissue

Fig. 9. The effects of human loading on the standard planar monopole antenna. (a) Boresight gain. (b) Reflection coefficient.

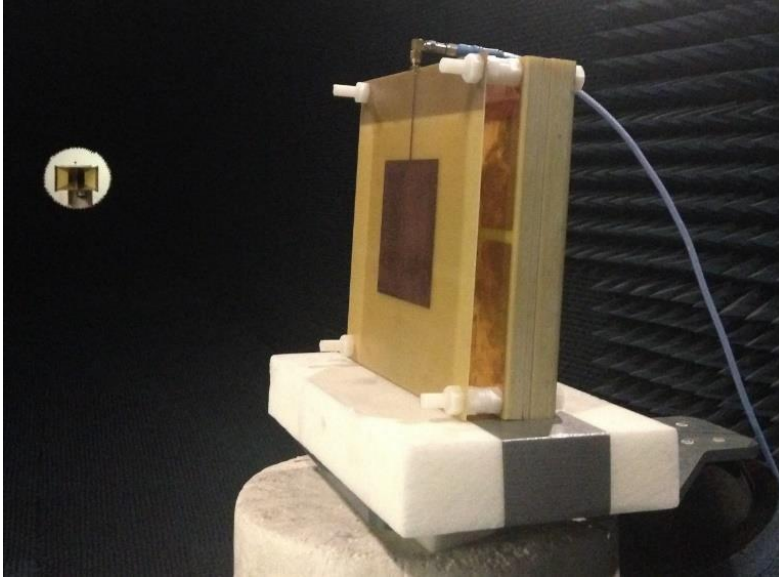


Fig. 10. (a) A picture of the loaded planar monopole antenna in the anechoic chamber.

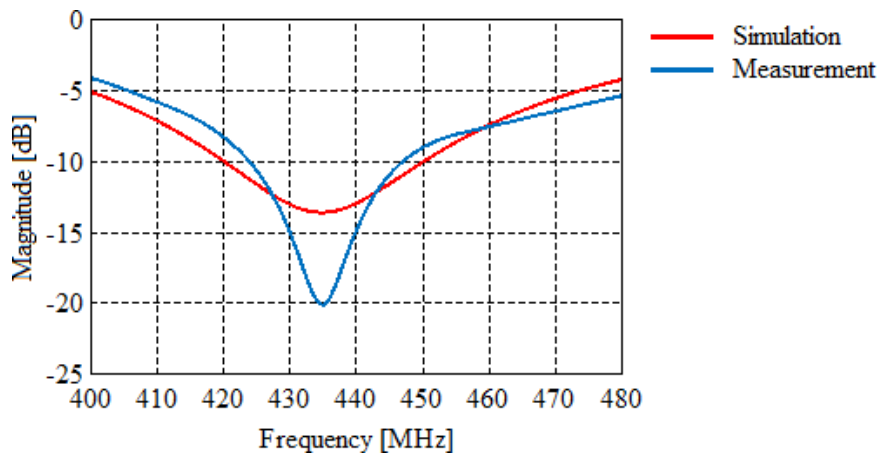


Fig. 10. (b) A comparison between the measured and simulated reflection coefficients for the loaded planar monopole antenna.

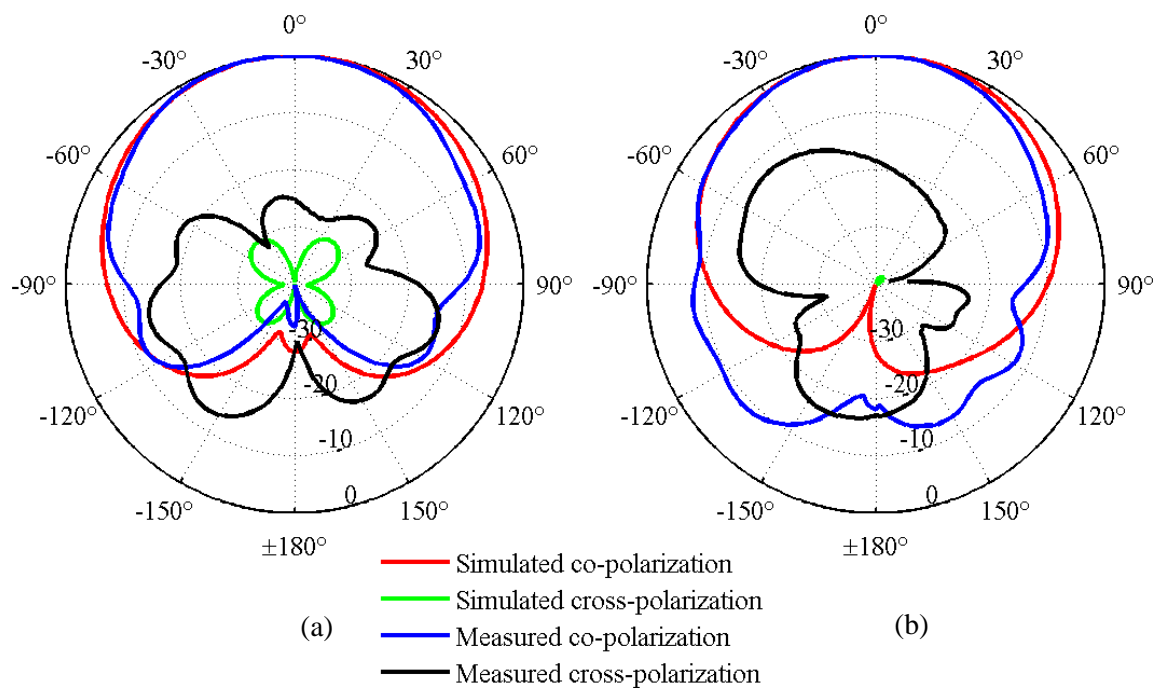
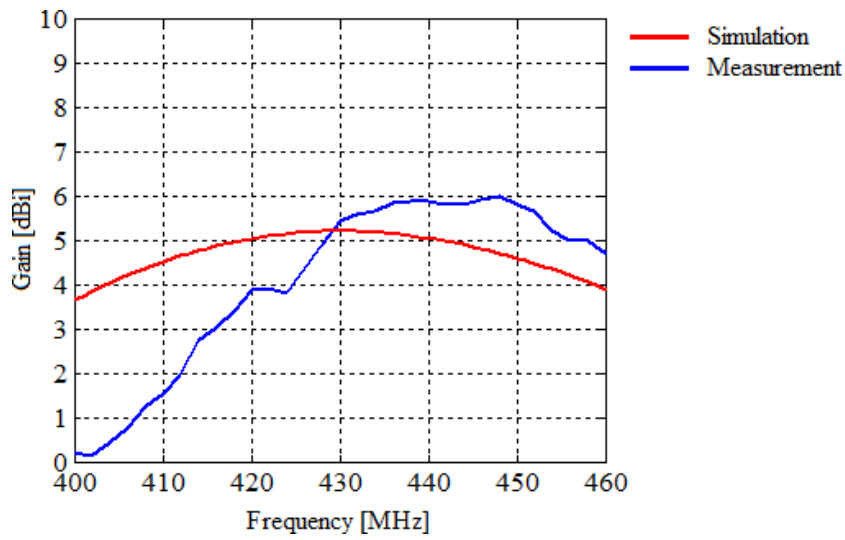
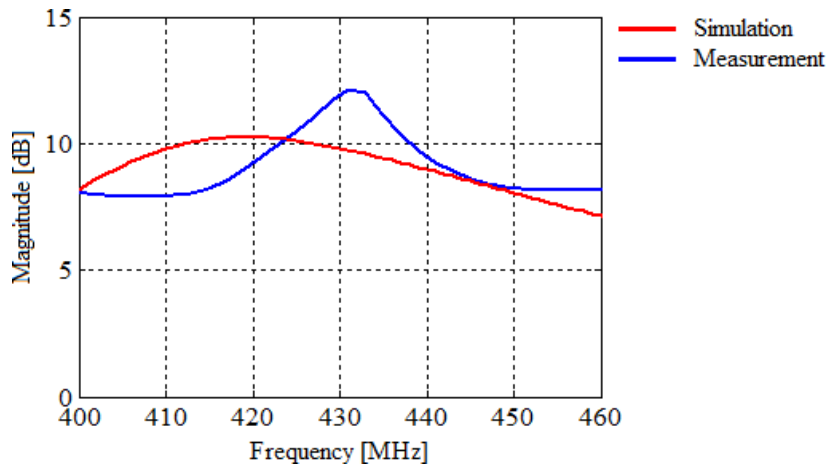


Fig. 11. Measured and simulated normalized radiation patterns for the loaded planar monopole antenna, (a) H-plane and, (b) E-plane radiation patterns.

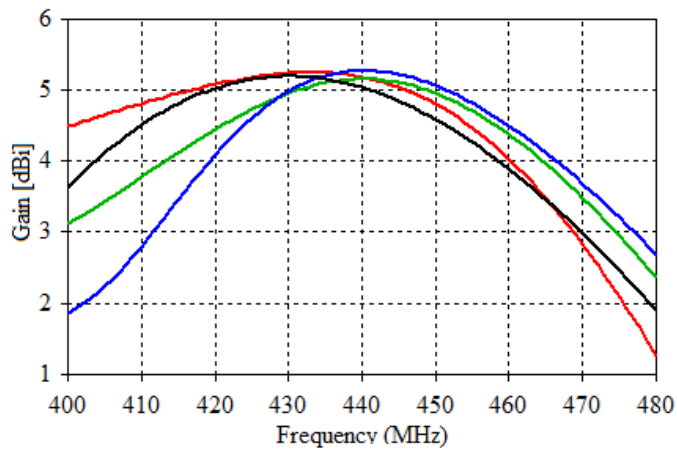


(a)

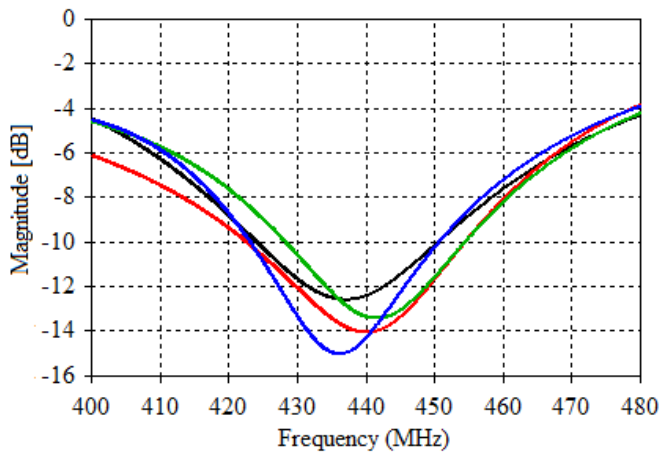


(b)

Fig. 12 (a). Measured and simulated boresight gain and (b) front to back power ratio for the loaded planar monopole antenna. The front to back power ratio is calculated as the ratio between the average power radiated towards the front hemisphere, relative to the average power radiated towards the rear hemisphere.



(a)



(b)

- human distance = 0.1 mm
- human distance = 20.0 mm
- human distance = 40.0 mm
- no human tissue

Fig. 13. The effects of human loading on the loaded planar monopole antenna. (a) Boresight gain and (b) Reflection coefficient.

TABLE I

FINAL STANDARD PLANAR MONOPOLE ANTENNA DESIGN PARAMETER VALUES

PARAMETER	VALUE IN MM
Antenna length (La)	205.65
Antenna width (W)	3
Ground length (gnd)	69.33
Square side length (Ls)	119.20
Space between squares (g)	19.45
Height of RIS (h)	38.4
Distance between antenna and RIS	8

TABLE II

FINAL LOADED PLANAR MONOPOLE ANTENNA DESIGN PARAMETER VALUES

PARAMETER	VALUE IN MM
Antenna length (La)	106.83
Antenna width (Wa)	106.83
Feed length (Lf)	68.95
Feed width (Wf)	3
Ground length (gnd)	37.77
Square side length (Ls)	110.89
Space between squares (g)	8.8
Height of RIS (h)	38.4
Distance between antenna and RIS	34

TABLE III
HUMAN TISSUE MODEL PROPERTIES [3]

LAYER	DIELECTRIC CONSTANT	CONDUCTIVITY (S/M)	DENSITY (KG/M ³)	LAYER THICKNESS (MM)
Skin	37.95	1.49	1001	2
Fat	5.27	0.11	900	10
Muscle Layer 1	52.67	1.77	1006	30
Bone	18.49	0.82	1008	20
Muscle Layer 2	52.67	1.77	1006	60